RSC Applied Polymers

ROYAL SOCIETY OF CHEMISTRY

PAPER

View Article Online
View Journal | View Issue

Cite this: *RSC Appl. Polym.*, 2024, **2**, 957

Oil-in-oil droplet stability dependence on dimensions of 2D Pickering particles of controlled size†

Simon D. Dale,[a] James Beament,[b] Andrew P. Dove *[a] and Rachel K. O'Reilly *[a]

Received 12th March 2024,
Accepted 7th July 2024

DOI: 10.1039/d4lp00091a

rsc.li/rscapplpolym

Non-aqueous emulsions are employed for a host of important applications; however, their long-term stability often limits their use. 2D particles have been reported to provide greater emulsion stability compared to surfactants and isotropic particles as a result of their greater interfacial area interaction. Here, control over the particle size resulted in control over the droplet diameter and increased stability. Non-aqueous emulsions are widely employed; therefore, characterising the effect of the dimensions of 2D particles on their stability is key to making oil-in-oil (o/o) emulsions with enhanced properties. This study investigates the self-assembly of uniform 2D particles of a controlled size, and their application as Pickering particles in o/o emulsions. The correlation between 2D particle dimensions and emulsion characteristics was investigated, a comparison that has not been reported for o/o emulsions prior to this study.

Introduction

Emulsions that do not contain an aqueous phase have seen an increase in interest in recent years due to their unique properties and applications.[1] The absence of an aqueous phase has been pivotal in the study of water-sensitive functionalities that otherwise would not be accessible in emulsion technology. Oil-in-oil (o/o) emulsions have a wide range of applications, from polymer synthesis to pharmaceutical development.[2] For example, polymeric particles, of a well-defined size, can be synthesised using water-sensitive catalysts and avoiding water-initiated degradation to undesired side products.[3–5] In the drive for achieving new and improved pharmaceuticals, o/o emulsions have enabled the study of new drugs that were either water sensitive or poorly soluble. This has aided their administration and, in some cases, their residence time.[6–8] For example, the encapsulation of ibuprofen was demonstrated to be greater in an o/o emulsion compared to a water containing emulsion.[9] With these ever expanding, and important, roles of o/o emulsions, they are seen as an exciting field for new developments.

Emulsifier choice plays a key role in the properties of the resulting emulsion, including stability or the droplet size. Control over such properties has previously proven difficult compared to water containing emulsions, due to the much lower interfacial tension between two oil phases.[1,2] Pickering particles have demonstrated many benefits over block copolymers (BCPs) and small molecule surfactants as emulsifiers. The solid particles require much higher energies to remove them from a liquid–liquid interface, whilst providing greater steric resistance to droplet coalescence.[10,11] Among this class of emulsifying agents, there are particular benefits in the use of 2 dimensional (2D) particles as a consequence of their high aspect ratio. This large surface area, and their expected orientation to lay with their edge parallel to the liquid–liquid interface, makes them even less likely to desorb compared to spherical or cylindrical particles.[12] The most common 2D materials that have been studied as Pickering particles are clay platelets[13–16] and graphene oxide (GO) nanosheets.[8,17,18] However, the preparation of these particles lacks any significant control over the dimensions of the resulting 2D emulsifier, which may be limiting their ability to control aspects of the emulsion such as stability or the droplet size. Therefore, to date, there has been no investigation into the role that the particle size plays in the properties of oil-in-oil (o/o) emulsions. Previously, our group demonstrated the important role 2D particle dimensions play in the droplet size and stability of water-in-water (w/w) emulsions.[19] Uniform PLLA-based diamond platelets with a larger surface area provided greater stability

[a]*School of Chemistry, University of Birmingham, Edgbaston, Birmingham, B15 2TT, UK. E-mail: a.dove@bham.ac.uk, r.oreilly@bham.ac.uk*
[b]*Infineum UK Ltd., Milton Hill, Abingdon, OX13 6BB, UK*

†Electronic supplementary information (ESI) available: Polymer synthesis, self-assembly, characterisation of nano-objects, emulsion methods and analysis. See DOI: https://doi.org/10.1039/d4lp00091a

and a smaller droplet size compared to smaller platelets of the same chemistry and width.

BCP self-assembly is a well-studied method of nanoparticle synthesis. Of particular note, crystallisation-driven self-assembly (CDSA) has been reliably demonstrated to assemble anisotropic particles, including 2D platelets.[20] Control over the platelet size can be achieved by a process termed living CDSA: the epitaxial growth of a BCP unimer and, in some cases, a crystalline homopolymer to uniform "seed" particles created from the sonication of particles with high size dispersity.[21] The size of the resulting platelets can be controlled through the mass ratio between the seed particles and the added unimer and semi-crystalline homopolymer. This process was first reported by Eisenberg and co-workers, where the addition of the poly(ε-caprolactone) (PCL) homopolymer to the assembly of PCL–PEO drove a morphological ripening of 1D cylinders to 2D platelet particles.[22] This has recently been improved upon as a method of obtaining PCL-based platelets of a uniform size by a living growth mechanism, demonstrating robust control over the particle dimensions.[23]

Given the importance of o/o emulsions, the development of emulsifiers that can be tuned to provide emulsions with defined properties would be a significant achievement. Considering the previously observed dependency of droplet stability on particle size for w/w emulsions, we postulated that a similar dependence would be observed in o/o emulsions. We therefore investigated a living CDSA methodology of 2D particle synthesis in nonpolar solvents to generate platelets of different sizes with low size dispersity. These platelets were used as emulsifiers to investigate the dependency of droplet properties on the dimensions. To directly compare the effects of particle dimension control with previous reports, we replicated the same systems that employed GO sheets of high size dispersity as emulsifiers: a dispersed phase of *N*,*N*-dimethylformamide (DMF) within a continuous phase of octane in a 1/5 ratio.[17] As octane is the continuous phase, particle formation would be conducted in this solvent prior to the addition of DMF. Particles of two sizes were investigated as emulsifiers at varying platelet concentrations. The droplet size was observed to differ significantly from the comparable study, and a droplet stability dependency on the platelet size was observed at a certain concentration.

Results and discussion

PCL has been widely studied as a core forming block for CDSA, with reports demonstrating its ability to form 2D particles of a controlled size, mostly taking place in water.[23] As a biocompatible and biodegradable aliphatic polyester, PCL has been of great interest for pharmaceutical and biological applications.[24,25] Hence, utilising PCL as the base of these Pickering particles, compared to GO, increases the potential applications in the biological field. The biodegradability of the PCL core may also offer opportunities to control degradation and hence release from emulsions, thus highlighting the potential advantages of using PCL-containing particles as Pickering stabilizers.

Log P_{oct} solubility calculations normalised to the surface area (log P_{oct}/SA) demonstrated a significant difference in solubility parameters between PCL (log P_{oct}/SA = 0.010) and octane (log P_{oct}/SA = 0.022), suggesting this would be a suitable core forming block for self-assembly in octane. As methacrylates with linear alkyl sidechains are reported as steric stabilising blocks for a range of *n*-alkane soluble nanoparticles, this type of polymer was investigated as a soluble stabilising block.[26–28] From log P_{oct} calculations, poly(*n*-decyl methacrylate) (P*n*DMA) possessed a closely matching hydrophobicity to that of octane (log P_{oct}/SA = 0.023); therefore this was selected as the stabilising block for this study.

A PCL_{50} macro-CTA was targeted using a bifunctional ring-opening polymerisation (ROP) initiator and a reversible-addition fragmentation chain transfer (RAFT) agent as previously reported (Fig. S1 & S2†).[29] A degree of polymerisation (DP) of 50 was achieved after 6 h with a narrow dispersity ($Đ_M$ = 1.07) (Scheme S1, Fig. S3 & S4†). RAFT polymerisation of *n*DMA using the PCL_{50} macro chain transfer agent (CTA) provided the amphiphilic BCP PCL_{50}-*b*-P*n*DMA_{155} after 18 h as determined by ^{1}H NMR spectroscopy (Scheme S1, Fig. S5 & S6†).

Size exclusion chromatography (SEC) analysis indicated good control over the polymerisation, with a narrow dispersity of molecular weight ($Đ_M$ = 1.16) observed (Fig. S7†). Good agreement of the refractive index (RI) and UV (λ = 309 nm) indicated retention of the trithiocarbonate end group in the purified product. The semi-crystallinity of the PCL block was maintained in the di-block as observed through thermal analysis by differential scanning calorimetry (DSC), providing a melting temperature (T_m) of 49.5 °C, a crystallisation temperature (T_c) of −54.6 °C, and a glass transition temperature (T_g) of −64.9 °C (Fig. S8†). The retention of the semi-crystallinity of the PCL block, along with the hydrophobic nature of the methacrylate block, indicates that this BCP should be suitable to undergo CDSA in octane. Transmission electron microscopy (TEM) imaging of a solution of the polymer after self-assembly provided evidence that cylindrical particles had formed as targeted (Fig. S9A†). As controlled crystallisation into anisotropic nanoparticles had been demonstrated, we moved to the next stages of creating 2D particles of a controlled size *via* a living CDSA mechanism (Scheme 1A). Sonication of the cylindrical micelle solution resulted in the formation of seed particles with an average length (L_{ave}) of 54 ± 15 nm (Fig. S9B & C†). These seed particles were subsequently used to form platelets through the addition of a blend of the dissolved PCL_{50}-*b*-P*n*DMA_{155} unimer and the PCL_{50} homopolymer. The mass ratio of the unimer to PCL_{50} was set at 1 (m_{unimer}/m_{PCL50} = 1) for all living growth experiments, whilst the mass ratio of seeds and the unimer (m_{unimer}/m_{seed}) was varied from 1, 10, 25, 40 to 100. Atomic force microscopy (AFM) analysis provided images of platelets at each of these m_{unimer}/m_{seed} ratios, with the size of the platelet increasing as m_{unimer}/m_{seed} increased (Fig. 1A–E & S10†). The linear relationship between m_{unimer}/m_{seed} and the average platelet area demonstrates the controlled

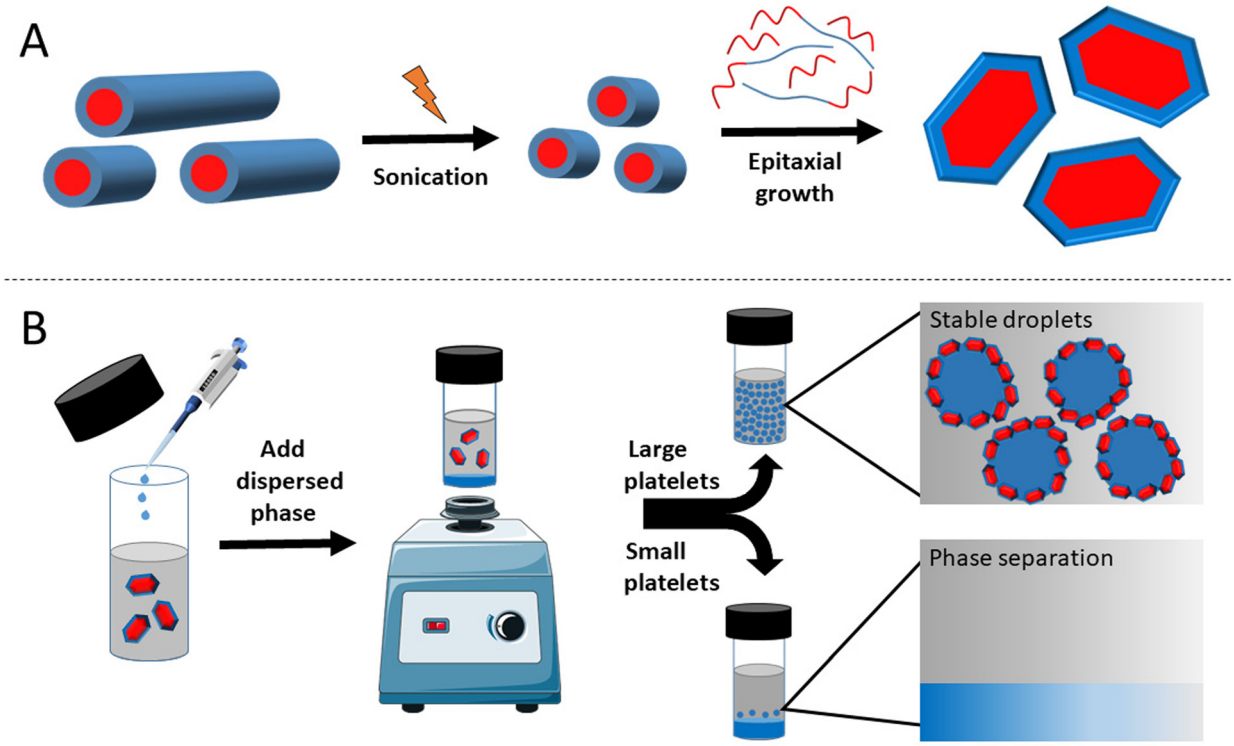

Scheme 1 (A) Mechanism of living CDSA to achieve 2D particles of a controlled size through the sonication of particles with high size dispersity to form "seeds" from which epitaxial growth of the unimer and the semi-crystalline homopolymer can take place. (B) Formation of emulsions using 2D particles by the addition of the dispersed phase to the platelet solution which, upon mixing, only forms stable emulsions when using emulsifiers with larger dimensions.

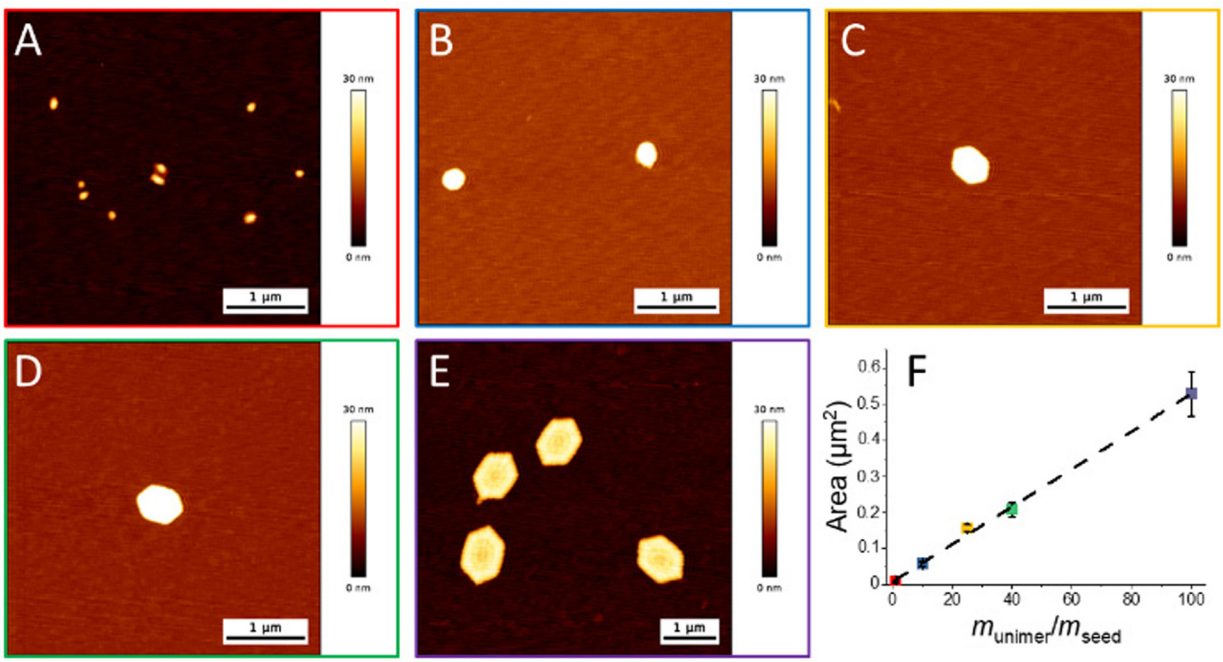

Fig. 1 AFM images of 2D platelets formed by the addition of PCL_{50} and PCL_{50}-*b*-P*n*DMA_{155} to seed particles at m_{unimer}/m_{seed} ratios (A) 1, (B) 10, (C) 25, (D) 40, and (E) 100 (F) Relationship between the m_{unimer}/m_{seed} ratio and the platelet area, 100 particles counted. Error bars represent standard deviation.

nature of the platelet size increase, meaning that the aim of achieving low dispersity platelets of defined dimensions was achieved (Fig. 1F). Control over the lateral dimensions was achieved; however, the width of the platelets remained constant. Therefore, the shape factor of the resulting platelets changes with increasing epitaxial growth. Alterations of the platelet width can be made through altering the BCP composition;[23] however, this was not considered for this study. The thickness of 2D Pickering stabilisers can have an effect on the emulsion, for example, increasing the density of clay platelets leads to destabilisation and, therefore, a less stable emulsion.[30] We therefore only altered the lateral dimensions of the platelets used in this study.

Given the fact that the control over the 2D particle size had been achieved, the ability of these particles to act as emulsifiers was investigated. Two platelet sizes were selected for this: m_{unimer}/m_{seed} = 25 (**P25**, platelet area = 0.15 ± 0.01 μm, Fig. 1C) and 100 (**P100**, platelet area = 0.53 ± 0.06 μm, Fig. 1E). These were chosen as they possessed significantly different areas; therefore any changes in the resulting emulsions would likely be as a result of the difference in the platelet area. We selected DMF, an aprotic polar solvent with a boiling point >100 °C, as the dispersed phase. As described earlier, the ability to use emulsions where both phases are stable at temperatures >100 °C unlocks the possibility to use emulsion technology for applications that would not be possible when one of the phases is water. After the addition of DMF (octane/DMF = 5/1 v/v), the solutions were vortexed for 30 seconds (Scheme 1B). The concentration of platelets in octane was varied as the platelet concentration has been demonstrated to play a role in droplet stability, and it was therefore of great interest to determine the effect of altering this variable on droplet properties.

After vortexing the solutions containing 1% w/w platelets (Fig. S11†), both sizes of platelets provided stable emulsions with a consistent droplet size over 4 weeks (Fig. S12–S14, and Table S1†). Interestingly, the droplet size did not appear to be dependent on the platelet dimensions, possibly as a consequence of the higher particle concentration compared to other systems.[17] Interestingly, the droplet size observed for these controlled emulsifier systems was significantly smaller than that using GO sheets using the same solvent system.[17] The droplet size has a direct influence on a range of emulsion properties including optics,[31] rheology,[32] pharmaceutical activity,[33] and stability.[34] Smaller droplets also benefit from longer stability times as a consequence of being more resistant to gravitational forces, leading to greater resilience against sedimentation or creaming.[34] The ability to produce smaller droplets can benefit these applications, as well as provide longer term stability in storage so that the properties remain consistent over time.[35]

Subsequently, the concentration of platelets of both sizes was reduced to 0.2% w/w in octane. As in the case when the concentration was 1% w/w, droplets with a relatively low size dispersity were observed, with the droplet diameter <6 μm on average (Fig. 2, Fig. S15 & S16, Table S2†). Analysis of the emulsion stabilised by P25 indicated good stability over 1 h. However, ripening was evident after this as the average droplet diameter steadily increased over the 3 day aging period (Fig. 2E, Fig. S15†). Long term instability of these emulsions was observed after 4 weeks of aging, with phase separation observed in the microscopy analysis (Fig. 2B). However, when imaging the emulsion of the same concentration of P100, no phase separation was observed after the same 4 week aging period (Fig. 2A & Fig. S16†). The droplet diameter remained relatively stable over this period, indicating that ripening was not taking place (Fig. 2E, Table S2†). These results demonstrate that the area of the platelet employed as the Pickering particle does indeed play an important role in droplet stability.

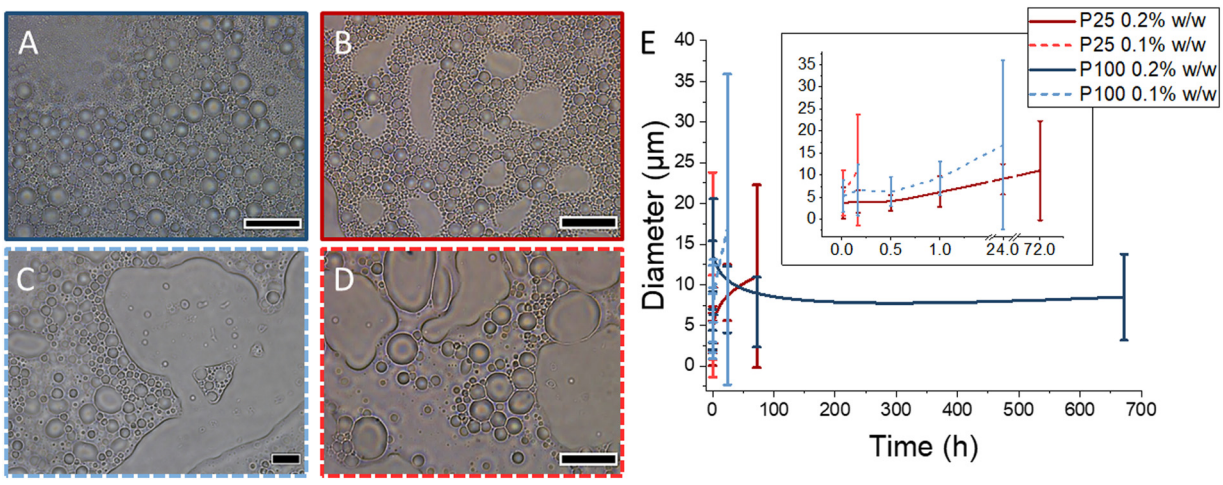

Fig. 2 (A) Microscopy images of emulsions using P100 as an emulsifier at 0.2% w/w after 4 weeks. (B) Microscopy images of emulsions using P25 as an emulsifier at 0.2% w/w after 3 days. (C) Microscopy images of emulsions using P100 as an emulsifier at 0.1% w/w after 24 h. (D) Microscopy images of emulsions using P25 as an emulsifier at 0.1% w/w after 10 minutes. (E) Evolution of emulsion diameters over time until phase separation; inset: emulsion diameters from 1 min to 3 days for emulsions with stability <4 weeks. All TEM scale bars = 50 μm.

After observing the long-term stability of the larger platelets at 0.2% w/w, a further concentration reduction to 0.1% w/w was tested using P100. The droplet size steadily increased over the first 1 h with some phase separation clearly observed when imaging after 24 h (Fig. 2C and E, Fig. S17†). Significantly larger areas of free solvent were present after 3 days, as phase separation continued over the longer aging period. However, in comparison, P25 only provided droplet stability for 1 minute at 0.1% w/w, as large ill-defined droplets caused by ripening were observed after 10 minutes and clear phase separation was observed after 30 minutes (Fig. 2D and E, Fig. S18†). This again evidenced the increased stability afforded by the larger platelet dimensions at the same concentration of the emulsifier.

These observations were further investigated by analysing how the presence of the particles affected the surface tension (ST) between the two solvents through drop shape analysis of DMF in the platelet solutions at 0.1 and 0.2% w/w (Fig. 3, Fig. S19†). As anticipated, a droplet of DMF in solutions that contained P25 reduced the surface tension to a lower extent than those in solutions that contained P100 (Fig. 3). Inherently, a lower surface tension reduces the surface free energy (ΔG) of an emulsified system, as demonstrated in the following equation:[36]

$$\Delta G = \sigma \Delta A$$

where σ (N m^{-2}) is the ST and ΔA (m^2) is the total interfacial area. As P100 lowers ST to a greater extent than P25, a more stable emulsion of lower energy is therefore created. Interestingly, there did not appear to be significant differences in ST between the two concentrations of platelets with the same size. P25 reduced surface tension to 1.63 ± 0.08 mN m^{-1} at 0.1% w/w and 1.64 ± 0.37 mN m^{-1} at 0.2% w/w concentration, down from 6.68 ± 0.37 mN m^{-1} without emulsifiers present. Similarly, both concentrations of P100 provided similar reductions in ST: 0.81 ± 0.11 at 0.1% w/w and 0.84 ± 0.11 mN m^{-1} at 0.2% w/w. The similarity in ST for the different concentrations of platelets with the same size was attributed to the smaller volume of DMF used in drop shape analysis. These results further highlight the important influence of the platelet size on the stability of dispersed droplets.

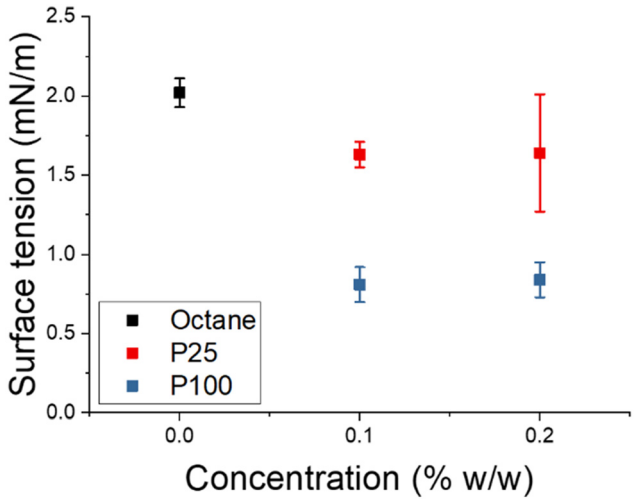

Fig. 3 Surface tension of a droplet of DMF in octane and solutions of platelets in octane at 0.2 and 0.1% w/w.

Additionally, the morphological dependency was further studied through changing the shape of the emulsifier. Short cylindrical particles of PCL_{50}-*b*-P*n*DMA_{155} were substituted for platelet particles as Pickering particles (Fig. S20†). Using the same emulsification strategy as above, at 0.2% w/w, emulsion droplets were observed after 1 minute; however phase separation was prevalent after only 2 minutes. Increasing the cylinder concentration up to even 4% w/w did not lead to stable emulsions over a long time period, as phase separation was observed after only 5 minutes. This demonstrates that the higher surface area results in platelets having a greater ability to sit at the interface and stabilise droplets compared to 1D particles.

To further expand the applicability of these emulsifiers, we investigated P100 as a stabiliser for a second polar non-aqueous solvent, acetonitrile (CH_3CN), in octane. Drop shape analysis of CH_3CN in solutions of P100 at 0.1 and 0.2% w/w demonstrated that the particles reduced ST from 1.35 ± 0.02 mN m^{-1} without particles to a similar level at both concentrations: 0.73 ± 0.38 and 0.53 ± 0.06 mN m^{-1} respectively (Fig. S21†). These reductions in ST resulted in emulsion droplets forming in the presence of P100 at 0.1 and 0.2% w/w following the same conditions as when DMF was the dispersed phase (Fig. S22†). These droplets were stable after 24 h, as no phase separation was observed at this timepoint. This result demonstrates the utility of these particles of a controlled size to act as stabilisers for multiple o/o systems, enhancing their applicability in the field of o/o emulsions.

Conclusions

It was demonstrated that the dimensions of 2D Pickering particles play a significant role in emulsion droplet stability. The controlled assembly of 2D platelets with a low size dispersity using PCL-based BCPs was achieved through matching of the solubility of an alkyl methacrylate corona block with the selected solvent by log P_{oct}/SA computational calculations. The epitaxial growth of the unimer and the semi-crystalline PCL_{50} homopolymer to seed particles was observed to provide 2D platelet particles of controlled dimensions. This is the first report of PCL-based BCPs assembling into 2D platelets of a controlled size in non-polar organic solvents, unlocking these materials to be implemented in many applications with the potential to be degradable post-use. Droplets of DMF in octane were stabilised over 4 weeks by platelets of two different sizes at a relatively high weight percentage; however, the droplet size was significantly smaller than that of a comparable study using GO sheets. This demonstrates the importance of the size of particles in how they act as Pickering stabilisers in non-

aqueous emulsions. A relationship between the platelet size and droplet stability was indicated, as the platelets with a larger size stabilised droplets to a greater extent compared to their smaller counterparts with the same chemistry. This highlights the potential advantages of controlling the dimensions of 2D particles as stabilisers for o/o emulsions, and this is an important consideration to make in any future formulations. We envisage that emulsion stability can be tailored to an application through simply altering the dimensions of the stabilising platelet. This system could therefore be utilised for timed release of the cargo, or to ensure that a desired reaction time can be achieved within the dispersed phase. Particles of this type are expected to find further use in emulsions for biological or environmental applications, as a consequence of the biologically compatible, and biodegradable, PCL core.

Author contributions

Conceptualisation: S. D. D., J. B., A. P. D., and R. K. O.; experimental data collection: S. D. D.; data analysis: S. D. D.; writing: S. D. D.; review and editing: S. D. D. and A. P. D.; supervision: A. P. D. and R. K. O.; funding acquisition: J. B.

Data availability

The datasets supporting this article have been uploaded as part of the ESI.†

Conflicts of interest

There are no conflicts to declare.

Acknowledgements

The authors would like to acknowledge funding from Infineum UK Ltd.

References

1 A. Zia, E. Pentzer, S. Thickett and K. Kempe, *ACS Appl. Mater. Interfaces*, 2020, **12**, 38845–38861.
2 D. Crespy and K. Landfester, *Soft Matter*, 2011, **7**, 11054–11064.
3 R. Dorresteijn, R. Haschick, M. Klapper and K. Müllen, *Macromol. Chem. Phys.*, 2012, **213**, 1996–2002.
4 C. Herrmann, D. Crespy and K. Landfester, *Colloid Polym. Sci.*, 2011, **289**, 1111–1117.
5 M. Klapper, S. Nenov, R. Haschick, K. Müller and K. Müllen, *Acc. Chem. Res.*, 2008, **41**, 1190–1201.
6 L. I. Atanase and G. Riess, *Int. J. Pharm.*, 2013, **448**, 339–345.
7 O. Suitthimeathegorn, J. A. Turton, H. Mizuuchi and A. T. Florence, *Int. J. Pharm.*, 2007, **331**, 204–210.
8 B. J. Rodier, A. de Leon, C. Hemmingsen and E. Pentzer, *Polym. Chem.*, 2018, **9**, 1547–1550.
9 Z. Mana, Y. Pellequer and A. Lamprecht, *Int. J. Pharm.*, 2007, **338**, 231–237.
10 R. Aveyard, B. P. Binks and J. H. Clint, *Adv. Colloid Interface Sci.*, 2003, **100–102**, 503–546.
11 B. P. Binks, *Curr. Opin. Colloid Interface Sci.*, 2002, **7**, 21–41.
12 P. Wei, Q. Luo, K. J. Edgehouse, C. M. Hemmingsen, B. J. Rodier and E. B. Pentzer, *ACS Appl. Mater. Interfaces*, 2018, **10**, 21765–21781.
13 N. P. Ashby and B. P. Binks, *Phys. Chem. Chem. Phys.*, 2000, **2**, 5640–5646.
14 B. Brunier, N. Sheibat-Othman, Y. Chevalier and E. Bourgeat-Lami, *Langmuir*, 2016, **32**, 112–124.
15 J. Dong, A. J. Worthen, L. M. Foster, Y. Chen, K. A. Cornell, S. L. Bryant, T. M. Truskett, C. W. Bielawski and K. P. Johnston, *ACS Appl. Mater. Interfaces*, 2014, **6**, 11502–11513.
16 X. Lu, J. S. Katz, A. K. Schmitt and J. S. Moore, *J. Am. Chem. Soc.*, 2018, **140**, 3619–3625.
17 B. Rodier, A. de Leon, C. Hemmingsen and E. Pentzer, *ACS Macro Lett.*, 2017, **6**, 1201–1206.
18 Y. He, F. Wu, X. Sun, R. Li, Y. Guo, C. Li, L. Zhang, F. Xing, W. Wang and J. Gao, *ACS Appl. Mater. Interfaces*, 2013, **5**, 4843–4855.
19 M. Inam, J. R. Jones, M. M. Pérez-Madrigal, M. C. Arno, A. P. Dove and R. K. O'Reilly, *ACS Cent. Sci.*, 2018, **4**, 63–70.
20 J. C. Foster, S. Varlas, B. Couturaud, Z. Coe and R. K. O'Reilly, *J. Am. Chem. Soc.*, 2019, **141**, 2742–2753.
21 L. MacFarlane, C. Zhao, J. Cai, H. Qiu and I. Manners, *Chem. Sci.*, 2021, **12**, 4661–4682.
22 G. Rizis, T. G. M. van de Ven and A. Eisenberg, *Angew. Chem., Int. Ed.*, 2014, **53**, 9000–9003.
23 Z. Tong, Y. Xie, M. C. Arno, Y. Zhang, I. Manners, R. K. O'Reilly and A. P. Dove, *Nat. Chem.*, 2023, **15**, 824–831.
24 L. S. Nair and C. T. Laurencin, *Prog. Polym. Sci.*, 2007, **32**, 762–798.
25 E. Chiellini and R. Solaro, *Adv. Mater.*, 1996, **8**, 305–313.
26 B. T. Seyrnour, R. K. E. Wright, A. C. Parrott, H. Y. Gao, A. Martini, J. Qu, S. Dai and B. Zhao, *ACS Appl. Mater. Interfaces*, 2017, **9**, 25038–25048.
27 L. A. Fielding, M. J. Derry, V. Ladmiral, J. Rosselgong, A. M. Rodrigues, L. P. D. Ratcliffe, S. Sugihara and S. P. Armes, *Chem. Sci.*, 2013, **4**, 2081–2087.
28 M. J. Derry, O. O. Mykhaylyk, A. J. Ryan and S. P. Armes, *Chem. Sci.*, 2018, **9**, 4071–4082.
29 Y. Su, Y. Jiang, L. Liu, Y. Xie, S. Chen, Y. Wang, R. K. O'Reilly and Z. Tong, *Macromolecules*, 2022, **55**, 1067–1076.
30 M. Vis, J. Opdam, I. S. J. van 't Oor, G. Soligno, R. van Roij, R. H. Tromp and B. H. Erné, *ACS Macro Lett.*, 2015, **4**, 965–968.
31 W. Chantrapornchai, F. Clydesdale and D. J. McClements, *Colloids Surf., A*, 1999, **155**, 373–382.
32 R. Pal, *AIChE J.*, 1996, **42**, 3181–3190.

33 M. Jaiswal, R. Dudhe and P. K. Sharma, *3 Biotech*, 2015, **5**, 123–127.
34 T. Tadros, P. Izquierdo, J. Esquena and C. Solans, *Adv. Colloid Interface Sci.*, 2004, **108–109**, 303–318.
35 S. Kumar, J. Ali and S. Baboota, *Nanotechnology*, 2016, **27**, 435101.
36 K. Schroën, J. de Ruiter and C. Berton-Carabin, *ChemEngineering*, 2020, **4**, 63.